Determining Invisible Particle Masses at the LHC

Hsin-Chia Cheng
U.C. Davis

NTU-UCDavis Physics Workshop,
From LHC to the Universe,
Dec. 15-18, 2008

Introduction

- New physics containing invisible particle(s) at the TeV scale is well-motivated.
  - WIMP dark matter
  - Precision electroweak constraints
- Many candidates for new physics at the TeV scale have some new parity symmetries. As a result, the lightest particle charged under the new symmetry will be stable, and can be a dark matter candidate if neutral. E.g., supersymmetry (R-parity) UEDs (KK-parity), little Higgs with T-parity, etc.

Introduction

- At colliders these models give similar signatures: jets/leptons + missing energy.
- To identify/distinguish the underlying new physics, we need to reconstruct the signal events and measure the properties of the new particles, including masses, spins and couplings. However, with 2 or more missing particles in each event, this is quite challenging.

LHC Theory Initiative White Paper

The LHC Theory Initiative: from the Standard Model to New Physics

October 24, 2005

The LHC-TI Steering Committee

Jonathan Bagger (Johns Hopkins University)

Ulrich Baur (State University of New York at Buffalo)

R. Sekhar Chivukula (Michigan State University)

Sarah Eno (University of Maryland)

Walter Giele (Fermi National Accelerator Laboratory)

JoAnne Hewett (Stanford Linear Accelerator Center)

Ian Hinchliffe (Lawrence Berkeley National Laboratory)

Paul Langacker [*Chair*] (University of Pennsylvania)

Steve Mrenna (Fermi National Accelerator Laboratory)

Fred Olness (Southern Methodist University)

Lynne Orr (University of Rochester)

John Parsons (Columbia University)

Martin Schmaltz (Boston University)

Carlos Wagner (Argonne National Laboratory and EFI, University of Chicago)

Edward Witten (Institute for Advanced Study, Princeton)

B.3.8 Prioritized List of Projects

Based on the discussion in the preceding sections, we prioritize the new physics projects of the LHC-TI as follows:

1. Needed at LHC startup (2007 – 2008):

   (a) study how the spin of SUSY particles and their couplings can be measured.

   (b) study the jet activity in cascade events.

   (c) include CP-violating phases in supersymmetric production and decay processes.

   (d) examine how well the sum rules of Little Higgs and Higgsless models can be tested as a function of the integrated luminosity available.

   (e) complete spin correlations in the RS model in `Pythia` and fully implement the UED in `Pythia` and `Herwig`. Calculate search reaches for UED.

   (f) develop benchmark points for models with extra dimensions and gather information on the parameter space which is consistent with existing data.

   (g) study the discovery reach of the LHC in Higgsless models with gauge-Higgs unification and Randall-Sundrum type models.

   (h) learn how well SUSY and UED can be discriminated.

Mass measurements from kinematics

- No invariant mass peak if there are missing particles.
- Most observables are sensitive to mass differences instead of overall mass scale.
- Total cross section and the likelihood method are model-dependent. One needs to know the model first.
- Goal: model-independent mass determinations from kinematics only.

Mass measurements from kinematics

Methods:

- End point/edge of invariant mass distributions
- New kinematic variables, e.g., M_{T2}
- Kinematic constraints from mass shell conditions

Experimental smearing, backgrounds, and combinatorics are important issues. We will focus on the methods in this talk and try to find features that are less sensitive to these potential problems.

End point method

Hinchliffe et al, hep-ph/9610544, and many others

Example: the dilepton edge.

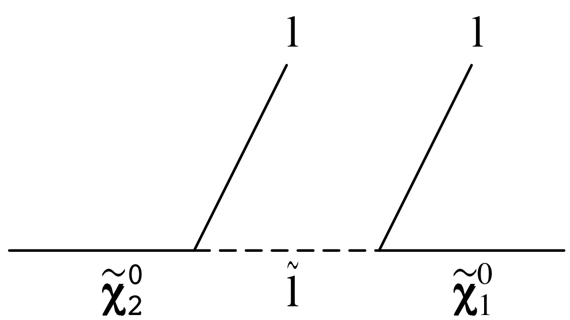

$$\text{Edge at } M_{ll} = \frac{\sqrt{(M^2_{\tilde{\chi}_2^0} - M^2_{\tilde{l}})(M^2_{\tilde{l}} - M^2_{\tilde{\chi}_1^0})}}{M_{\tilde{l}}}$$

- Requires longer decay chains.
- Does not use all information, e.g., the other chain.

End point method

Example:

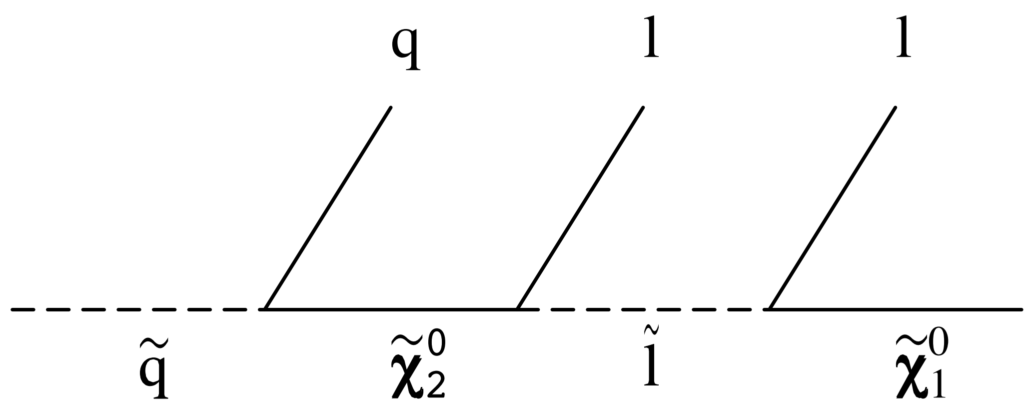

There are endpoints in the invariant mass distributions m_{ll}, m_{qll}, $m_{ql(high)}$, $m_{ql(low)}$.

SPS 1a study points:

Gjelsten, Miller, Osland, hep-ph/0410303

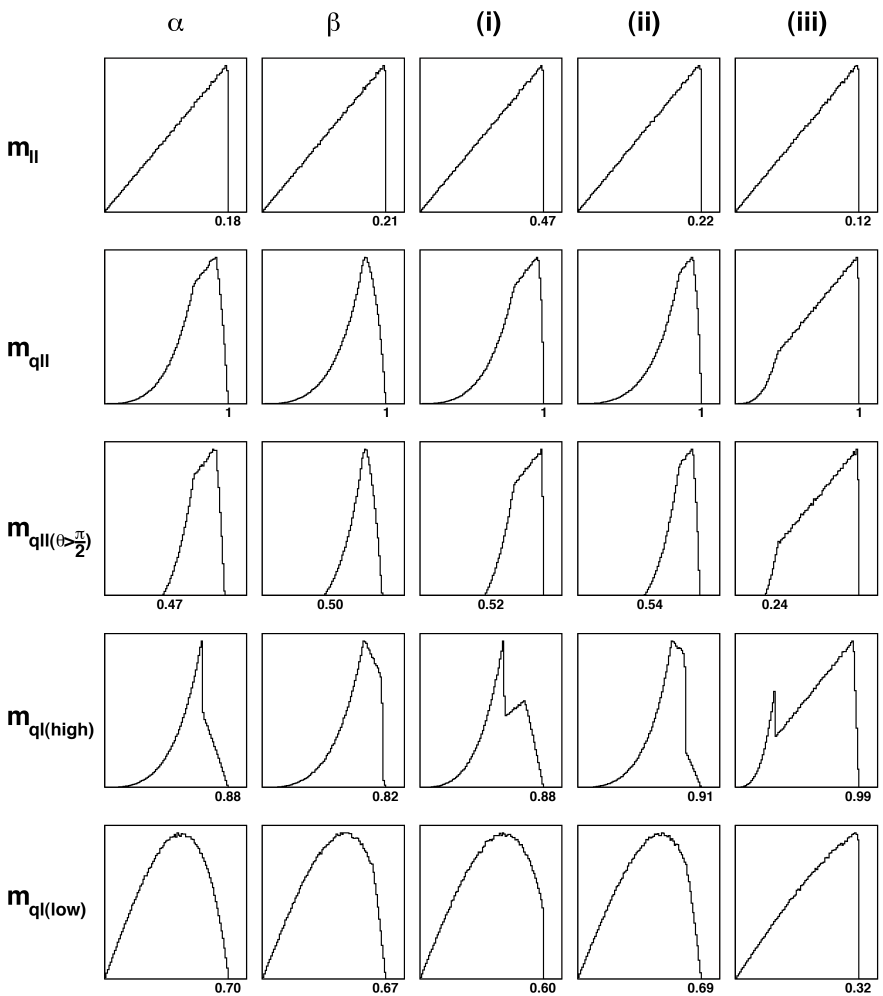

(i) $\tilde{g} > \max(\tilde{d}_L, \tilde{u}_L, \tilde{b}_1, \tilde{t}_1)$ and $\tilde{\chi}_2^0 > \max(\tilde{l}_R, \tilde{\tau}_1)$

(ii) $\tilde{g} > \max(\tilde{d}_L, \tilde{u}_L, \tilde{b}_1, \tilde{t}_1)$ and $\tilde{l}_R > \tilde{\chi}_2^0 > \tilde{\tau}_1$

(iii) $\tilde{g} > \max(\tilde{d}_L, \tilde{u}_L, \tilde{b}_1, \tilde{t}_1)$ and $\min(\tilde{l}_R, \tilde{\tau}_1) > \tilde{\chi}_2^0$

Point	$\tilde{g}$	$\tilde{d}_L$	$\tilde{d}_R$	$\tilde{u}_L$	$\tilde{u}_R$	$\tilde{b}_2$	$\tilde{b}_1$	$\tilde{t}_2$	$\tilde{t}_1$
(α)	**595.2**	**543.0**	520.1	**537.2**	520.5	**524.6**	**491.9**	574.6	379.1
(β)	**915.5**	**830.1**	799.5	**826.3**	797.3	**800.2**	**759.4**	823.8	610.4
	$\tilde{e}_L$	$\tilde{e}_R$	$\tilde{\tau}_2$	$\tilde{\tau}_1$	$\tilde{\nu}_{e_L}$	$\tilde{\nu}_{\tau_L}$		$H^\pm$	A
(α)	202.1	**143.0**	206.0	133.4	185.1	185.1		401.8	393.6
(β)	315.6	**221.9**	317.3	213.4	304.1	304.1		613.9	608.3
	$\tilde{\chi}_4^0$	$\tilde{\chi}_3^0$	$\tilde{\chi}_2^0$	$\tilde{\chi}_1^0$	$\tilde{\chi}_2^\pm$	$\tilde{\chi}_1^\pm$		H	h
(α)	377.8	358.8	**176.8**	**96.1**	378.2	176.4		394.2	114.0
(β)	553.3	538.4	**299.1**	**161.0**	553.3	299.0		608.9	117.9

Table 1: Masses [GeV] for the considered SPS 1a points (α) and (β) of Eq. (3.2).

$$(m_{ll}^{\max})^2 = \left(m^2_{\tilde{\chi}_2^0} - m^2_{\tilde{l}_R}\right)\left(m^2_{\tilde{l}_R} - m^2_{\tilde{\chi}_1^0}\right)/m^2_{\tilde{l}_R} \tag{4.3}$$

$$(m_{qll}^{\max})^2 = \begin{cases} \frac{\left(m^2_{\tilde{q}_L} - m^2_{\tilde{\chi}_2^0}\right)\left(m^2_{\tilde{\chi}_2^0} - m^2_{\tilde{\chi}_1^0}\right)}{m^2_{\tilde{\chi}_2^0}} & \text{for } \frac{m_{\tilde{q}_L}}{m_{\tilde{\chi}_2^0}} > \frac{m_{\tilde{\chi}_2^0}}{m_{\tilde{l}_R}}\frac{m_{\tilde{l}_R}}{m_{\tilde{\chi}_1^0}} \quad (1) \\ \frac{\left(m^2_{\tilde{q}_L} m^2_{\tilde{l}_R} - m^2_{\tilde{\chi}_2^0} m^2_{\tilde{\chi}_1^0}\right)\left(m^2_{\tilde{\chi}_2^0} - m^2_{\tilde{l}_R}\right)}{m^2_{\tilde{\chi}_2^0} m^2_{\tilde{l}_R}} & \text{for } \frac{m_{\tilde{\chi}_2^0}}{m_{\tilde{l}_R}} > \frac{m_{\tilde{l}_R}}{m_{\tilde{\chi}_1^0}}\frac{m_{\tilde{q}_L}}{m_{\tilde{\chi}_2^0}} \quad (2) \\ \frac{\left(m^2_{\tilde{q}_L} - m^2_{\tilde{l}_R}\right)\left(m^2_{\tilde{l}_R} - m^2_{\tilde{\chi}_1^0}\right)}{m^2_{\tilde{l}_R}} & \text{for } \frac{m_{\tilde{l}_R}}{m_{\tilde{\chi}_1^0}} > \frac{m_{\tilde{q}_L}}{m_{\tilde{\chi}_2^0}}\frac{m_{\tilde{\chi}_2^0}}{m_{\tilde{l}_R}} \quad (3) \\ \left(m_{\tilde{q}_L} - m_{\tilde{\chi}_1^0}\right)^2 & \text{otherwise} \quad (4) \end{cases} \tag{4.4}$$

$$(m^{\max}_{ql(\mathrm{low})}, m^{\max}_{ql(\mathrm{high})}) = \begin{cases} (m^{\max}_{ql_n}, m^{\max}_{ql_f}) & \text{for } 2m^2_{\tilde{l}_R} > m^2_{\tilde{\chi}_1^0} + m^2_{\tilde{\chi}_2^0} > 2m_{\tilde{\chi}_1^0}m_{\tilde{\chi}_2^0} \quad (1) \\ (m^{\max}_{ql(\mathrm{eq})}, m^{\max}_{ql_f}) & \text{for } m^2_{\tilde{\chi}_1^0} + m^2_{\tilde{\chi}_2^0} > 2m^2_{\tilde{l}_R} > 2m_{\tilde{\chi}_1^0}m_{\tilde{\chi}_2^0} \quad (2) \\ (m^{\max}_{ql(\mathrm{eq})}, m^{\max}_{ql_n}) & \text{for } m^2_{\tilde{\chi}_1^0} + m^2_{\tilde{\chi}_2^0} > 2m_{\tilde{\chi}_1^0}m_{\tilde{\chi}_2^0} > 2m^2_{\tilde{l}_R} \quad (3) \end{cases} \tag{4.5}$$

$$(m^{\max}_{ql_n})^2 = \left(m^2_{\tilde{q}_L} - m^2_{\tilde{\chi}_2^0}\right)\left(m^2_{\tilde{\chi}_2^0} - m^2_{\tilde{l}_R}\right)/m^2_{\tilde{\chi}_2^0} \tag{4.6}$$

$$(m^{\max}_{ql_f})^2 = \left(m^2_{\tilde{q}_L} - m^2_{\tilde{\chi}_2^0}\right)\left(m^2_{\tilde{l}_R} - m^2_{\tilde{\chi}_1^0}\right)/m^2_{\tilde{l}_R} \tag{4.7}$$

$$(m^{\max}_{ql(\mathrm{eq})})^2 = \left(m^2_{\tilde{q}_L} - m^2_{\tilde{\chi}_2^0}\right)\left(m^2_{\tilde{l}_R} - m^2_{\tilde{\chi}_1^0}\right)/\left(2m^2_{\tilde{l}_R} - m^2_{\tilde{\chi}_1^0}\right) \tag{4.8}$$

$$\begin{aligned}(m^{\min}_{qll(\theta>\frac{\pi}{2})})^2 = \Big[&\left(m^2_{\tilde{q}_L} + m^2_{\tilde{\chi}_2^0}\right)\left(m^2_{\tilde{\chi}_2^0} - m^2_{\tilde{l}_R}\right)\left(m^2_{\tilde{l}_R} - m^2_{\tilde{\chi}_1^0}\right) \\ &-\left(m^2_{\tilde{q}_L} - m^2_{\tilde{\chi}_2^0}\right)\sqrt{\left(m^2_{\tilde{\chi}_2^0} + m^2_{\tilde{l}_R}\right)^2\left(m^2_{\tilde{l}_R} + m^2_{\tilde{\chi}_1^0}\right)^2 - 16 m^2_{\tilde{\chi}_2^0} m^4_{\tilde{l}_R} m^2_{\tilde{\chi}_1^0}} \\ &+2m^2_{\tilde{l}_R}\left(m^2_{\tilde{q}_L} - m^2_{\tilde{\chi}_2^0}\right)\left(m^2_{\tilde{\chi}_2^0} - m^2_{\tilde{\chi}_1^0}\right)\Big]/\left(4m^2_{\tilde{l}_R} m^2_{\tilde{\chi}_2^0}\right)\end{aligned} \tag{4.9}$$

Gjelsten, Miller, Osland, hep-ph/0410303

$$\int \mathcal{L} dt = 300\, fb^{-1}$$

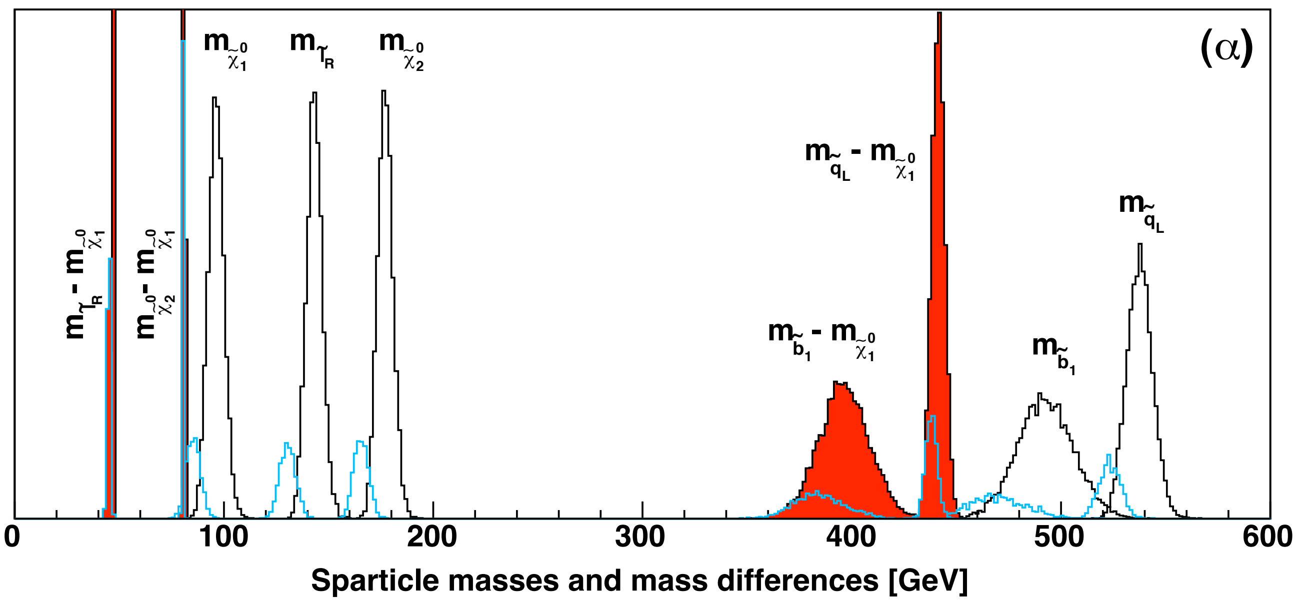

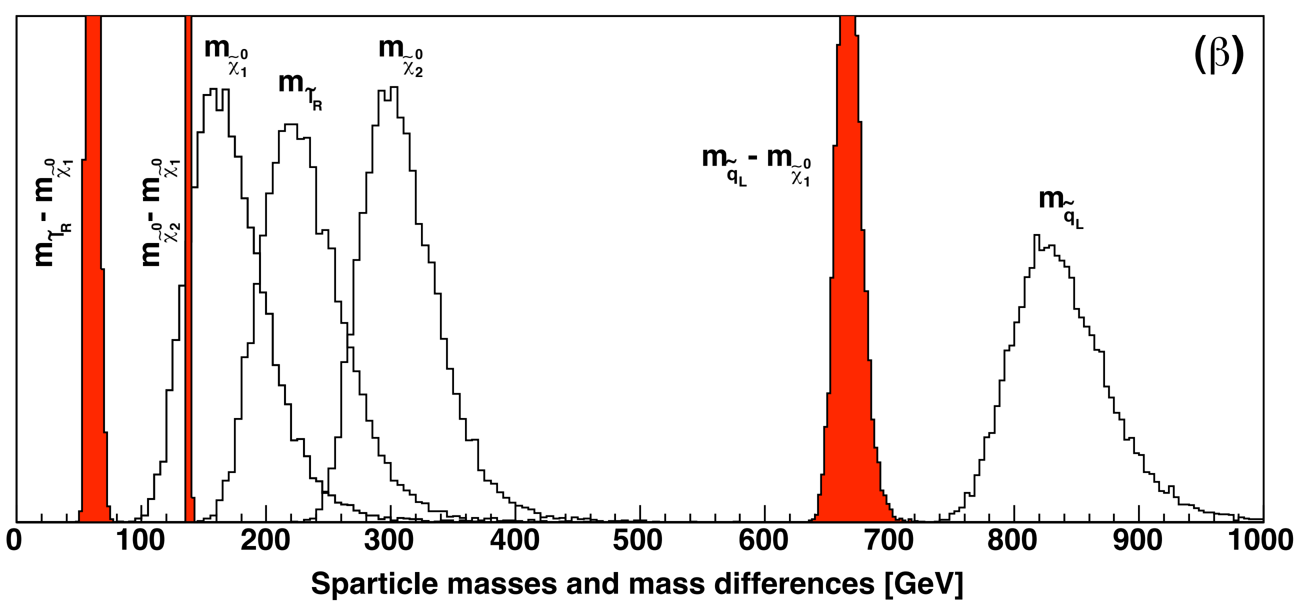

M_{T2} method

- Transverse mass M_T:

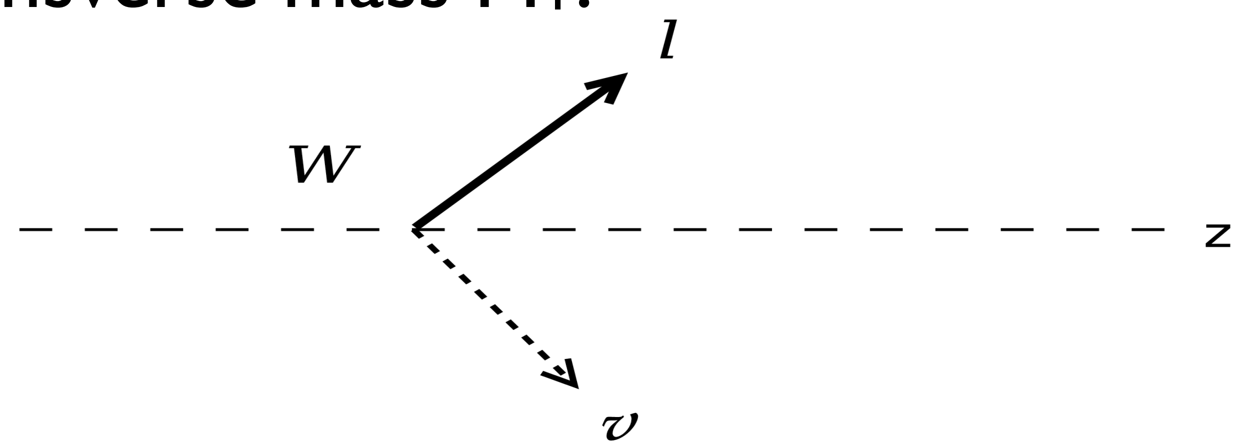

$$\alpha_\ell = (E_T^\ell, p_x^\ell, p_y^\ell), \quad \alpha_\nu = (E_T^\nu, p_x^\nu, p_y^\nu)$$

$$E_T^\ell = \sqrt{(p_x^\ell)^2 + (p_y^\ell)^2 + m_\ell^2}, \quad E_T^\nu = \sqrt{(p_x^\nu)^2 + (p_y^\nu)^2 + m_\nu^2}.$$

Transverse mass defined by

$$M_T^2 = (\alpha_\ell + \alpha_\nu)^2.$$

The end point of M_T distribution is M_W.

M_{T2} method

- Stransverse mass M_{T2}: Lester & Summers, hep-ph/9906349

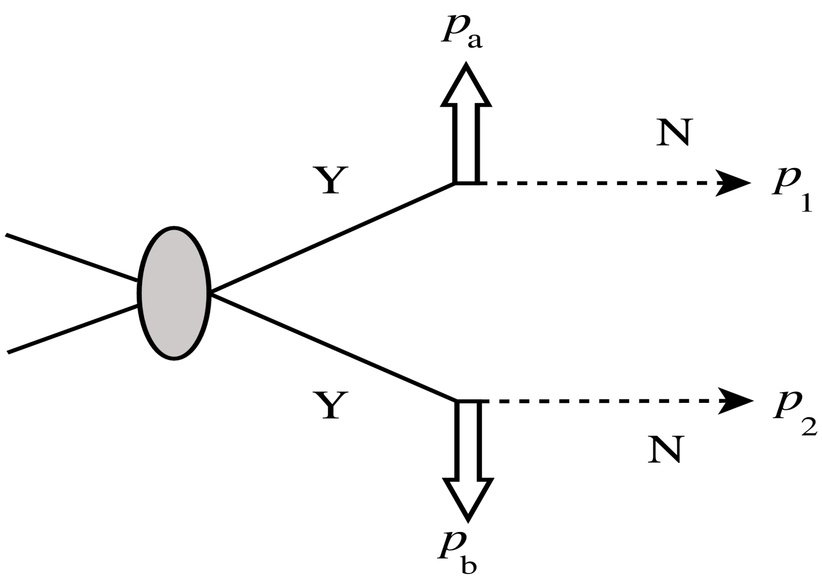

  - Trial N mass, μ_N
  - Consider all partitions of $\not{p}_T = \mathbf{p}_T^{(1)} + \mathbf{p}_T^{(2)}$.

$$M_{T2}(\mu_N) \equiv \min_{\mathbf{p}_T^{(1)} + \mathbf{p}_T^{(2)} = \not{\mathbf{p}}_T} \left[\max\{ M_T(1, a; \mu_N), M_T(2, b; \mu_N) \} \right]$$

M_{T2} method

Properties of M_{T2}:

- A function of the missing particle mass .
- End point of M_{T2} gives the correct mother particle mass M_Y if we assume the correct missing particle mass, $\mu_N = m_N$.

M_{T2} for an example event:

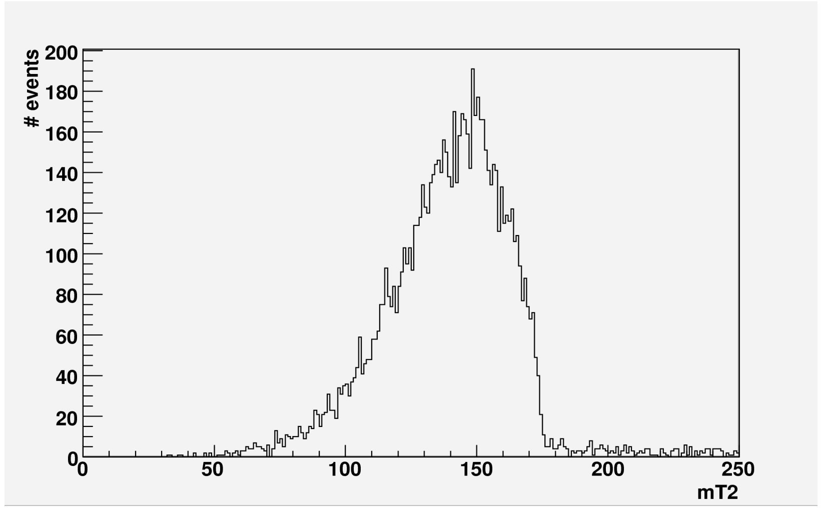

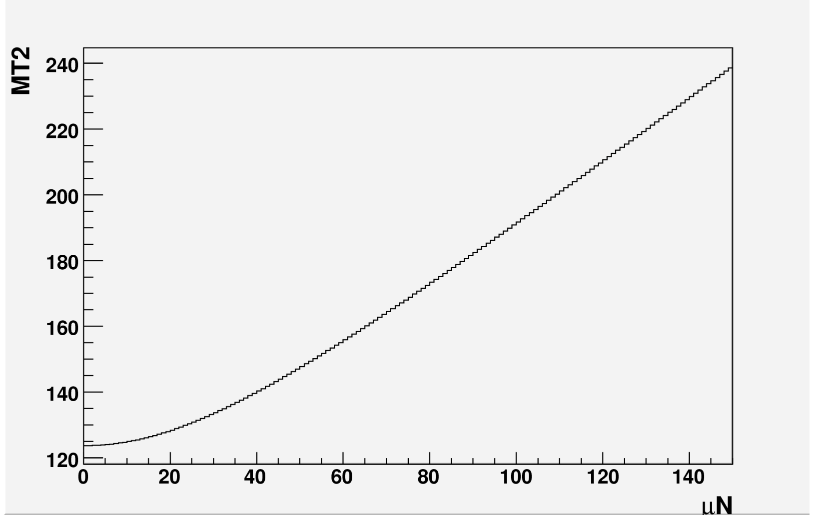

M_{T2} method

When there are 2 or more visible particles on each chain, $M_{T2,max}$ exhibits a kink at the correct mass point. Cho, et al, 0709.0288, 0711.4526

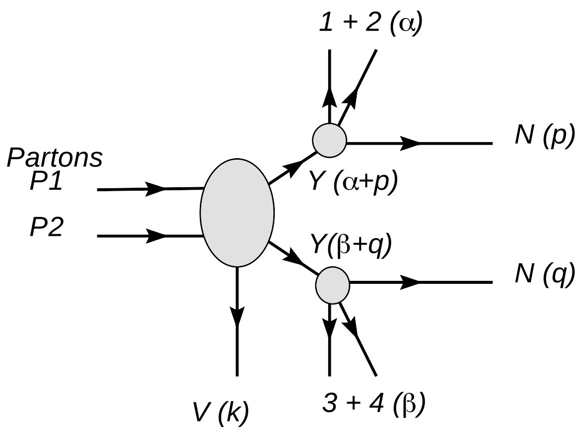

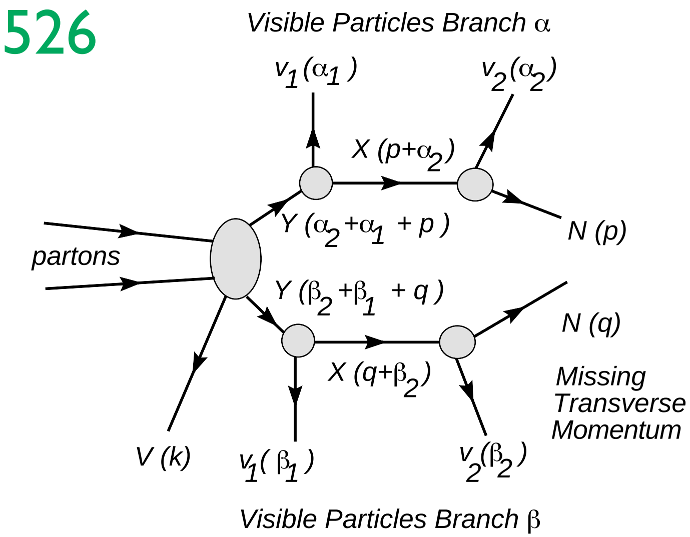

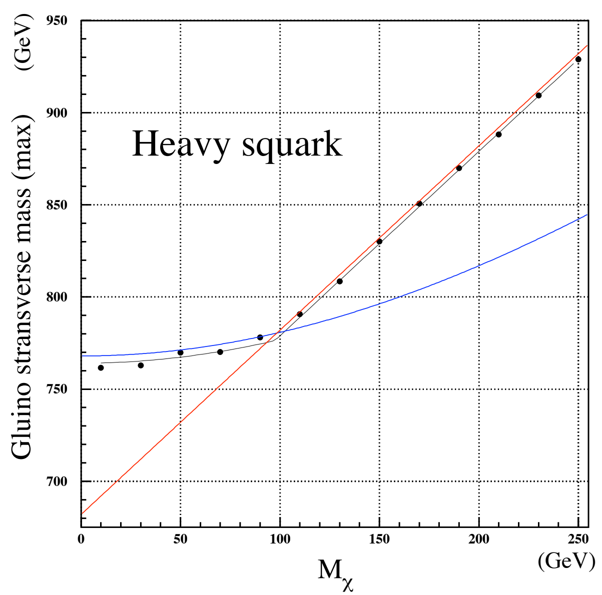

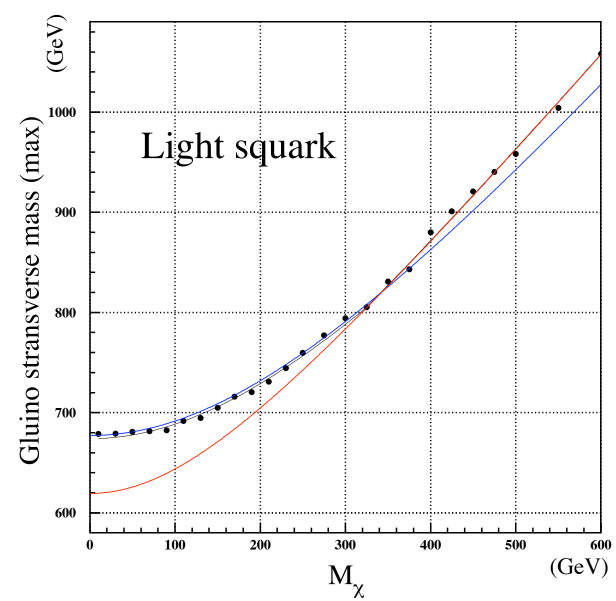

Kinematic constraints

- Find the allowed region in the mass parameter space for each event by imposing mass shell conditions.
- Find the intersection of allowed regions by combining many signal events.

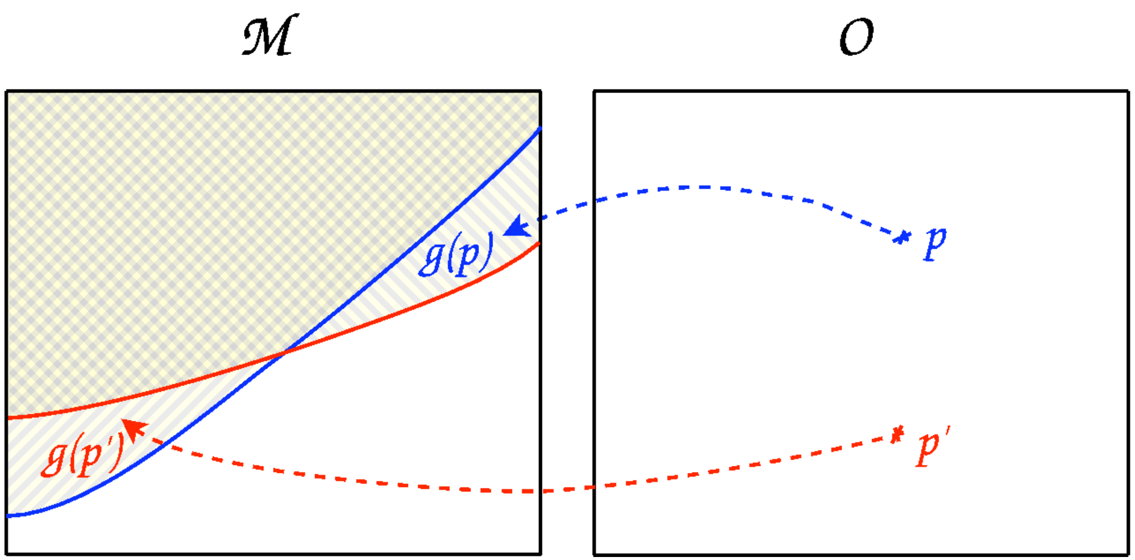

Kinematic constraints

- 3 visible particle per chain, e.g., $\tilde{q} \to q\tilde{\chi}_2^0 \to ql\tilde{l} \to qll\tilde{\chi}_1^0$

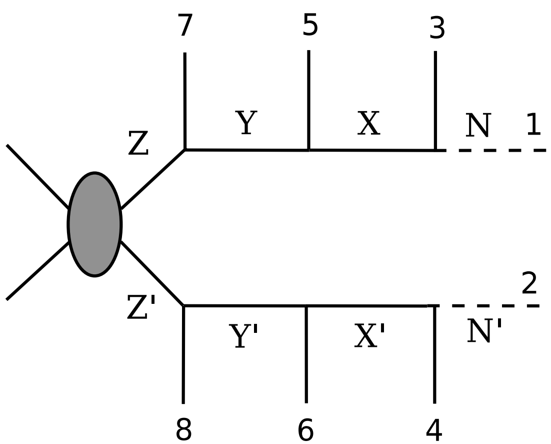

$$p_1^2 = p_2^2$$
$$(p_1 + p_3)^2 = (p_2 + p_4)^2$$
$$(p_1 + p_3 + p_5)^2 = (p_2 + p_4 + p_6)^2$$
$$(p_1 + p_3 + p_5 + p_7)^2 = (p_2 + p_4 + p_6 + p_8)^2$$
$$p_1^x + p_2^x = p_{miss}^x, \quad p_1^y + p_2^y = p_{miss}^y$$

HC, D. Engelhardt, J.F. Gunion, Z.Han, and B. McElrath, arXiv:0802.4290

- Can be solved by combining 2 events
- Combinatorial backgrounds are a serious issue. Need to find ways to reduce wrong combinations.

Example: $\tilde{q}\tilde{q} \rightarrow q\tilde{\chi}_2^0 q\tilde{\chi}_2^0 \rightarrow q\tilde{l}lq\tilde{l}l \rightarrow q\tilde{\chi}_1^0 llq\tilde{\chi}_1^0 ll$

SPS1a, masses: (97.4, 142.5, 180.3, 564.8) GeV

Ideal case

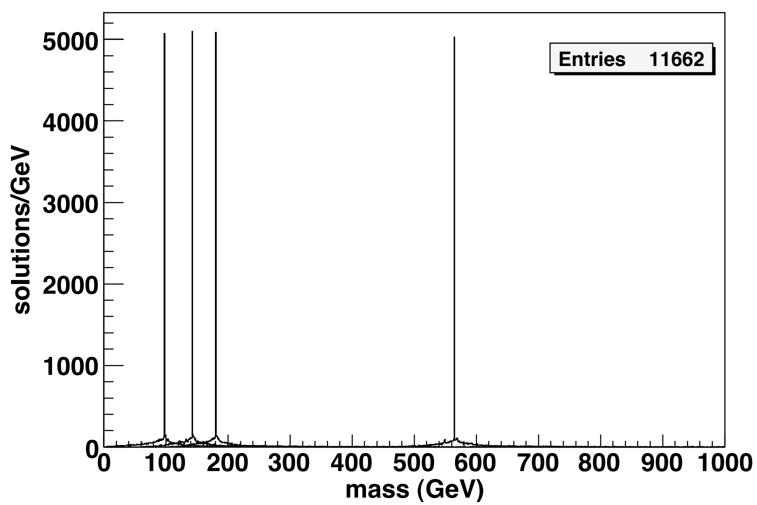

With wrong combinations

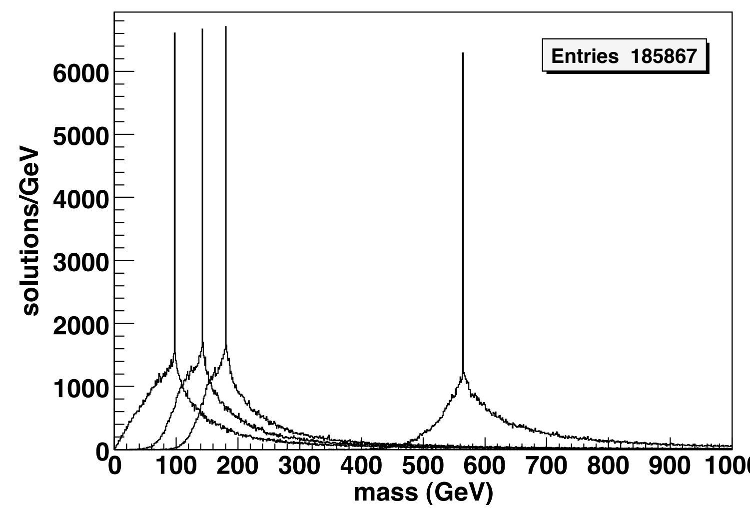

Including experimental smearing

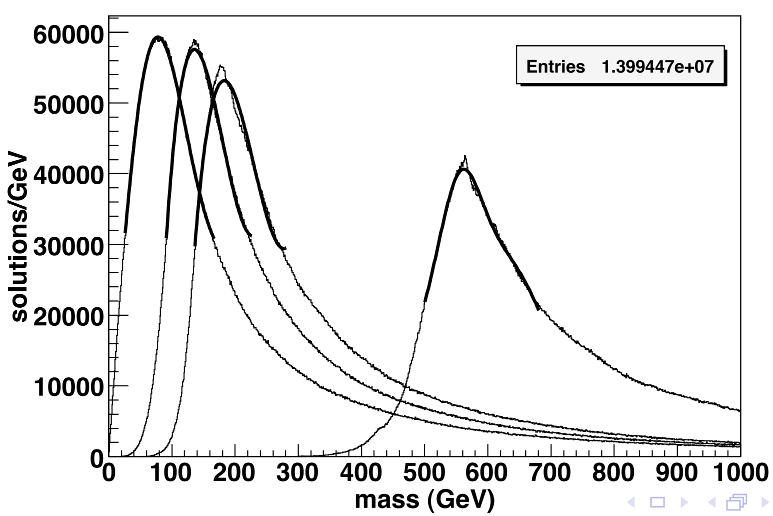

After background reduction

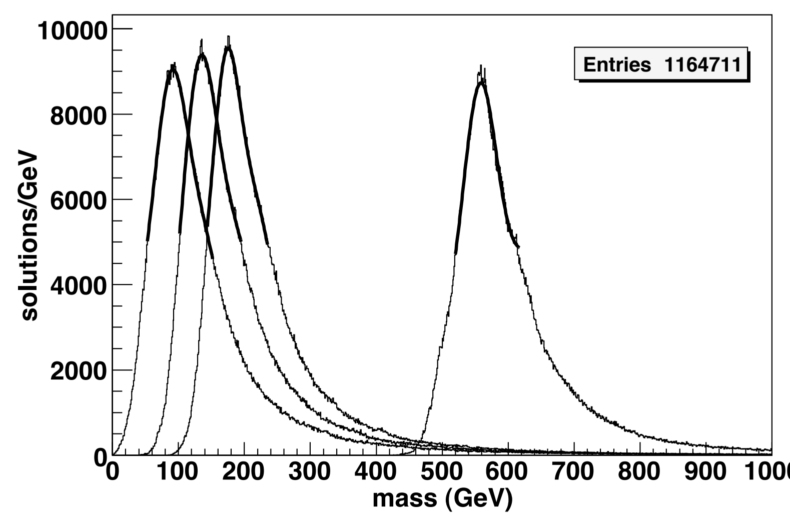

Kinematic constraints

- For shorter decay chains, the masses cannot be determined by kinematic constraints alone.

HC, J.F. Gunion, Z. Han, G. Marandella, and B. McElrath, arXiv: 0707.0030

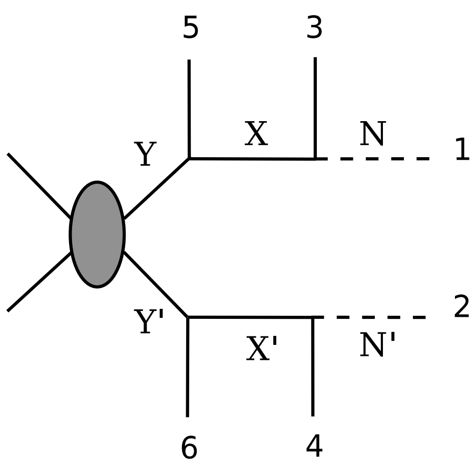

$(m_Y, m_X, m_N)=$ $(246.6, 128.4, 85.3)$ GeV
500 events, no smearing, correct combination

Consistent region, ideal case

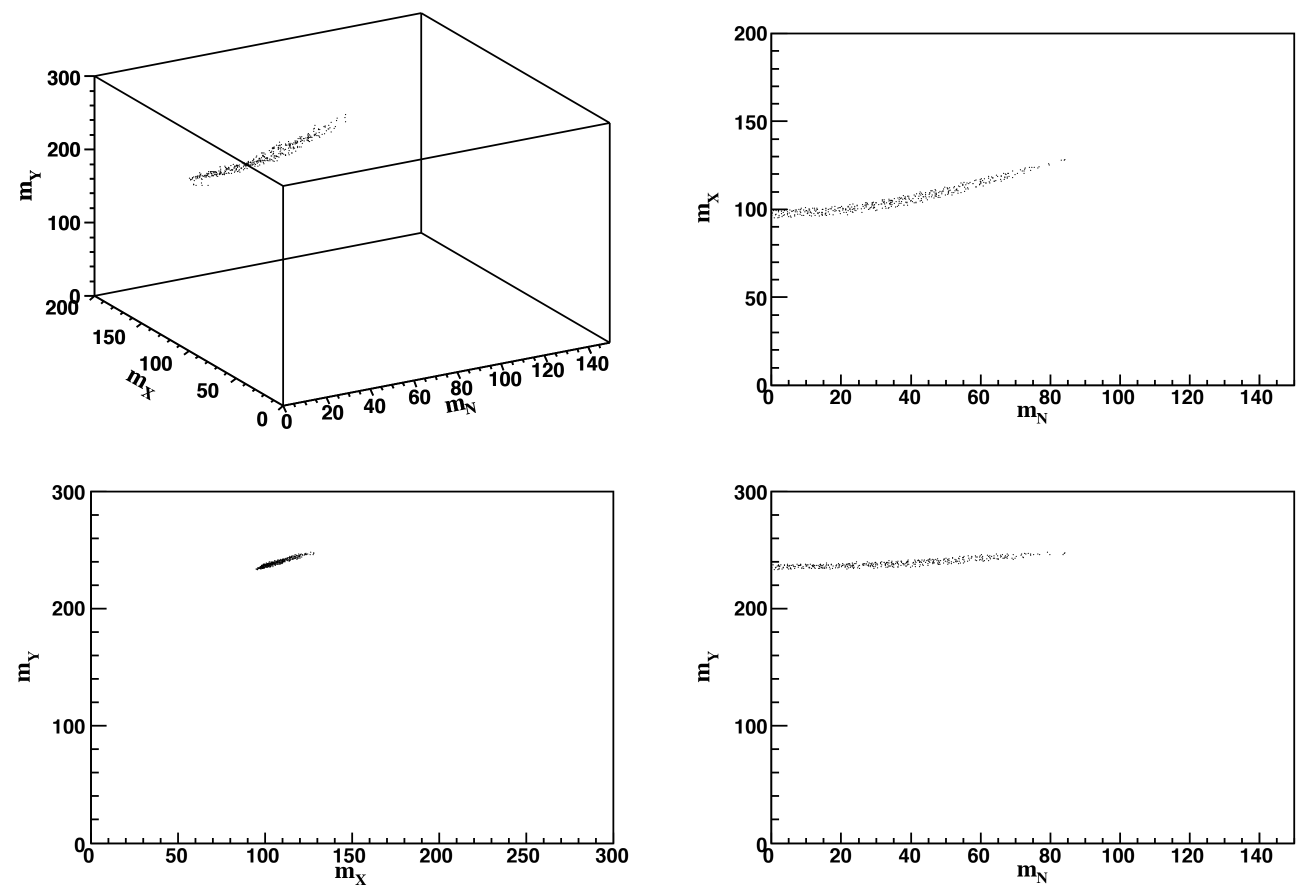

Minimal kinematic constraints and M_{T2}

HC and Zhenyu Han, arXiv:0810.5187

- Minimal kinematic constraints: mass shell constraints of the decaying mother particles and the missing particles + missing transverse momentum constraints

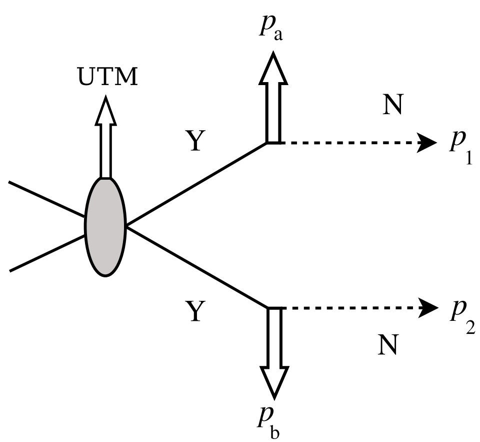

$$p_1^2 = p_2^2 = \mu_N^2,$$
$$(p_1 + p_a)^2 = (p_2 + p_b)^2 = \mu_Y^2,$$
$$p_1^x + p_2^x = \not{p}^x,\ p_1^y + p_2^y = \not{p}^y,$$

- $M_{T2}(m_N)$ is the boundary of the allowed region and forbidden region based on the minimal kinematic constraints.

Minimal kinematic constraints and M_{T2}

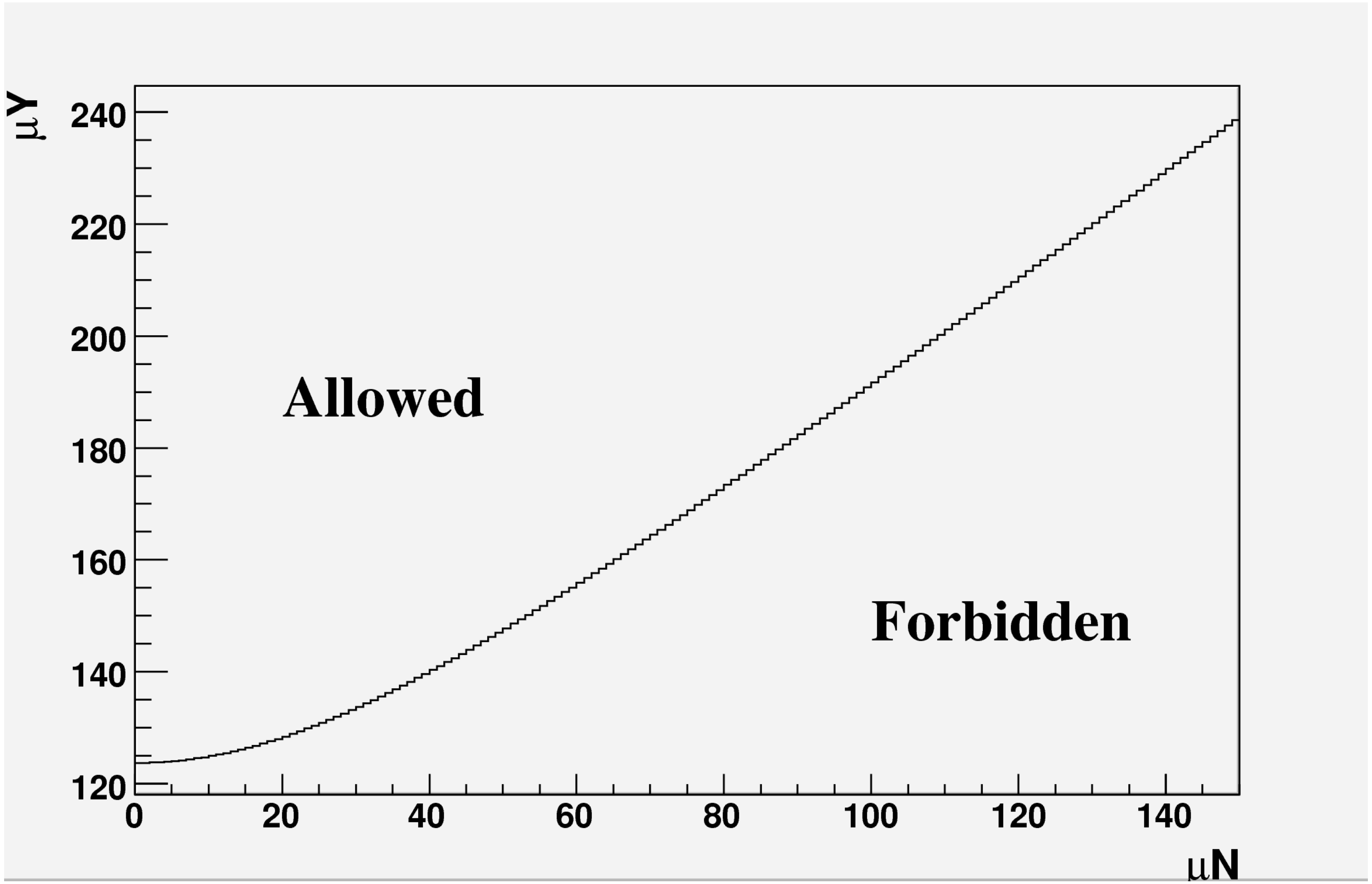

Based on this, we obtain a new way to calculate M_{T2}.

Calculating M_{T2}

- M_{T2} is the boundary of the allowed region, find the allowed region first.
- Consider one decay chain.

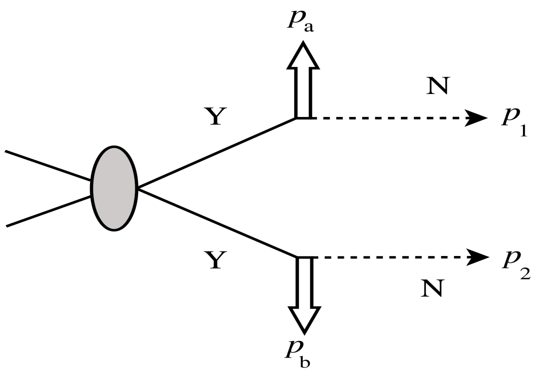

$$p_1^2 = \mu_N^2,$$
$$(p_1 + p_a)^2 = \mu_Y^2$$
$$\Rightarrow [E_1(p_{1x}, p_{1y}), p_{1x}, p_{1y}, p_{1z}(p_{1x}, p_{1y})].$$

- Require the momenta to be physical, the allowed (p_{1x}, p_{1y}) is within an ellipse. The ellipse expand when μ_Y increases. Minimum $\mu_Y = m_a + \mu_N$
- The other chain gives another ellipse, on (p_{2x}, p_{2y}) plain. But (p_{1x}, p_{1y}) and (p_{2x}, p_{2y}) related by missing momentum $\Longrightarrow$ Another ellipse on (p_{1x}, p_{1y}) plain
- Have solutions when two ellipses overlap.

Calculating M_{T2}

Unbalanced configuration

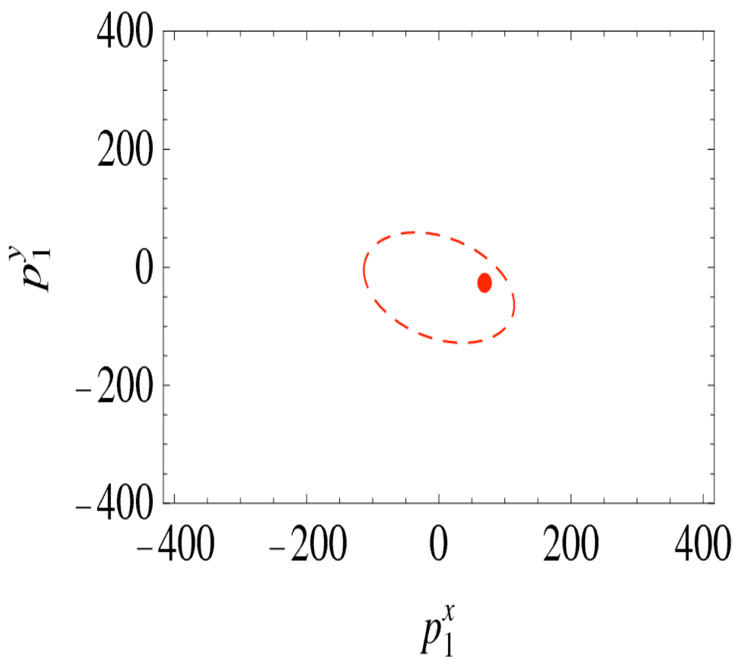

Balanced configuration

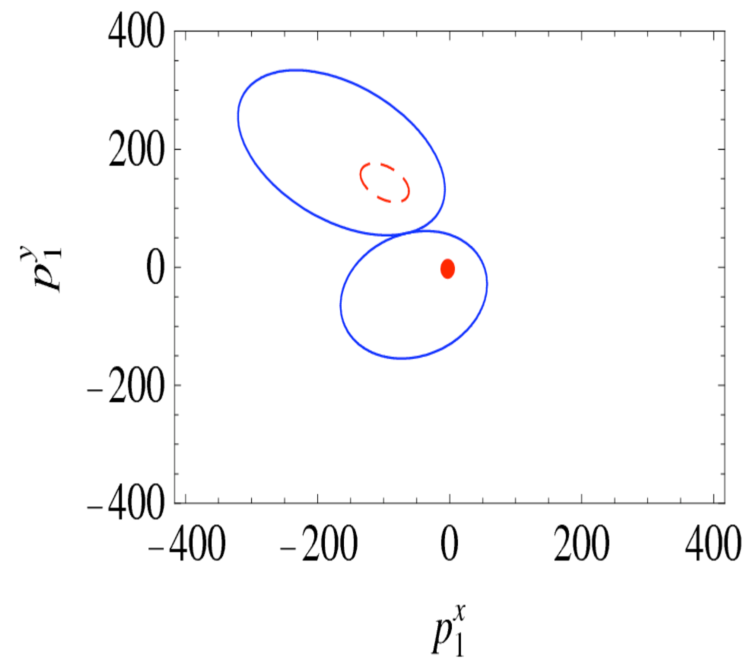

The new algorithm based on kinematic constraints is 5-9 time faster and more accurate than the previous available code (based on scanning and minimization).

Mass determination - hybrid method

Example 1:

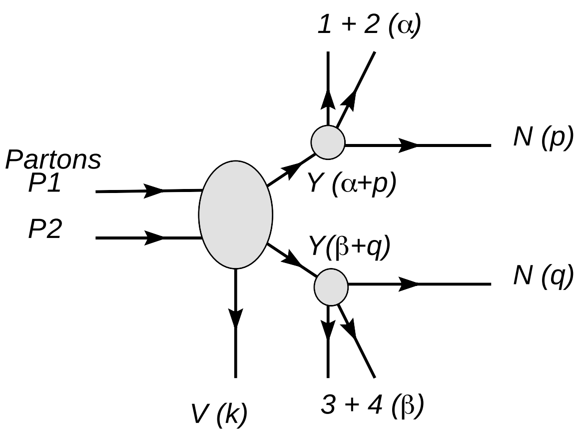

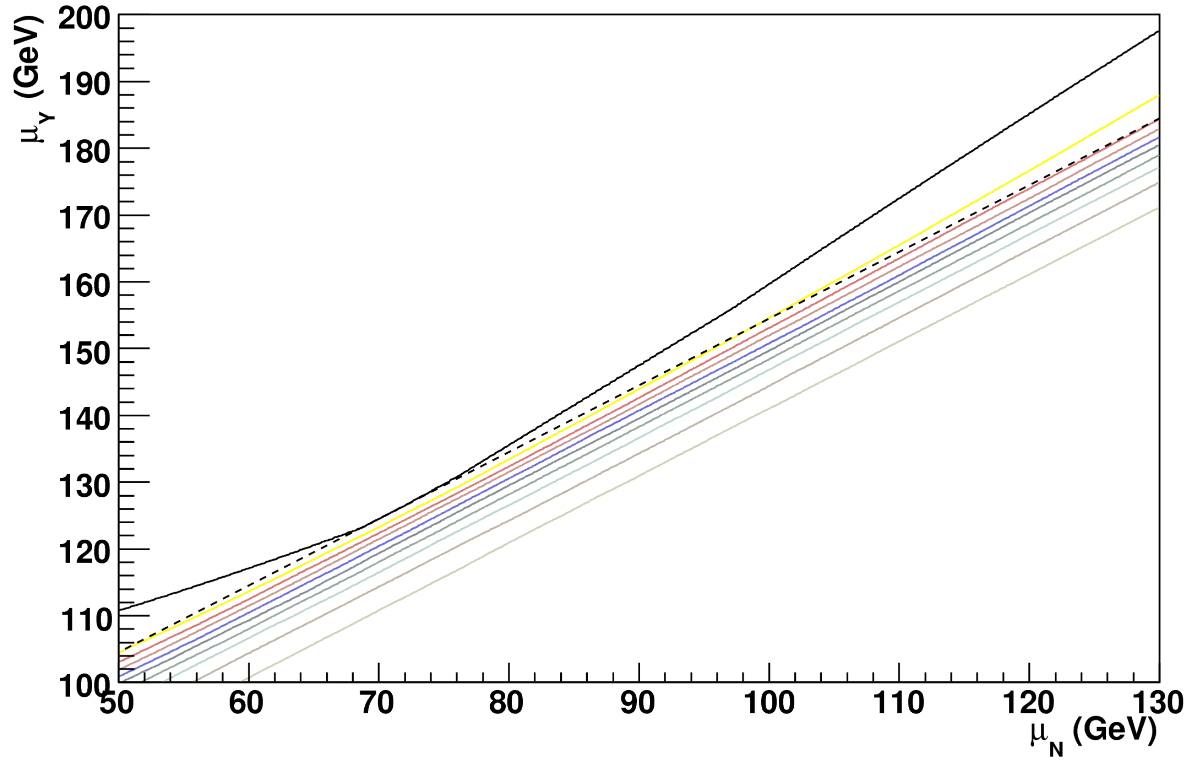

- Contours of # of solvable events. The top contour is the M_{T2} curve, which exhibit a kink.
- Dash line is the end point of the invariant mass of the visible particles in one chain (constant mass difference in this case).

Mass determination - hybrid method

If mass difference can be well-determined (only one chain is required, better statistics), one can count # of solvable events along the constant mass difference line. The correct mass is at maximum due to the kink nature of the contour.

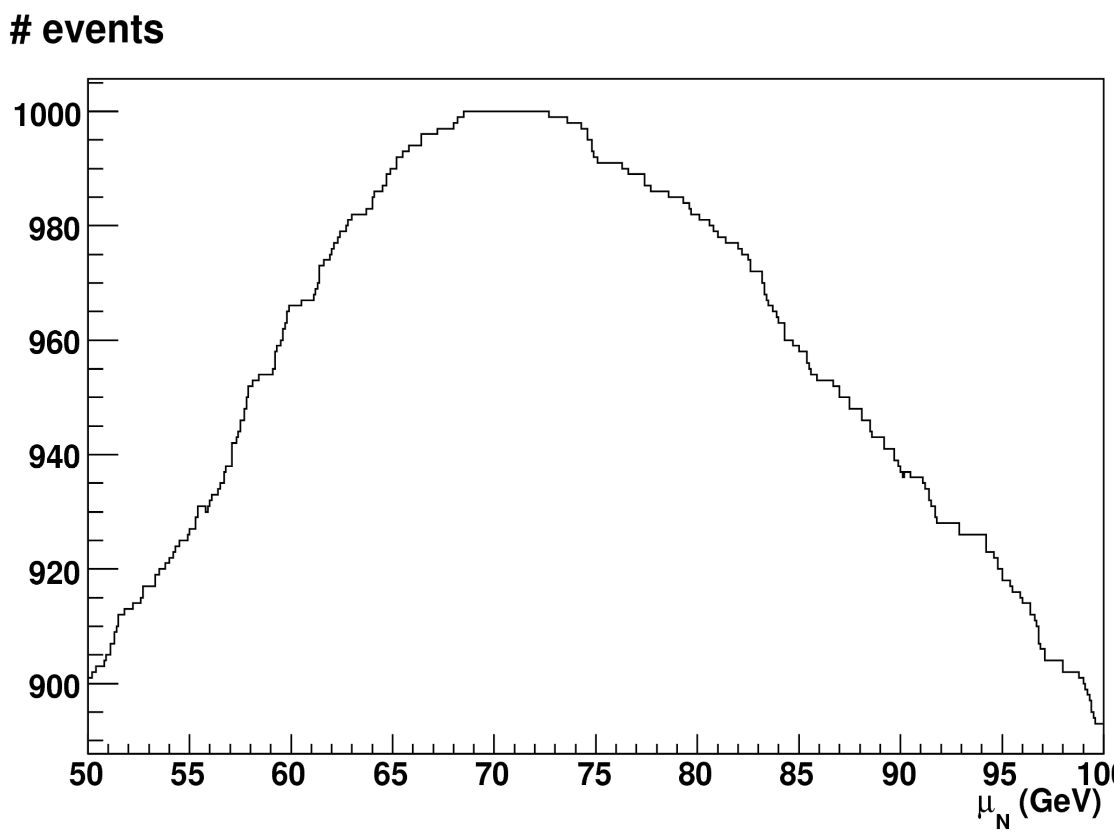

Mass determination - hybrid method

Example 2: on-shell intermediate particle

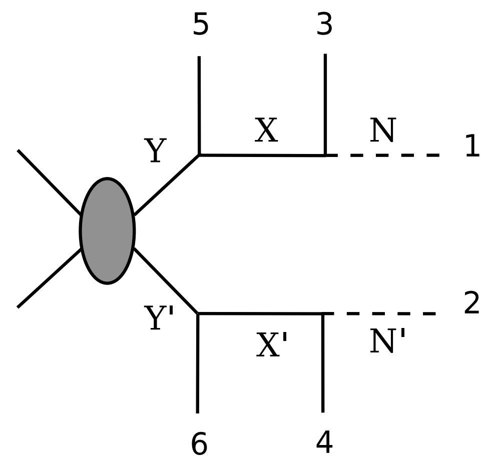

- First calculate M_{T2} end point contour, which relates m_Y and m_N.
- Another relation among m_Y, m_X, and m_N can be obtained from the end point of invariant mass,

$$m_{ll}\big|_{edge} = \frac{(M_Y^2 - M_X^2)(M_X^2 - M_N^2)}{M_X^2}$$

Mass determination - hybrid method

- Count # of solvable events along the contour by imposing the m_X mass shell constraint.

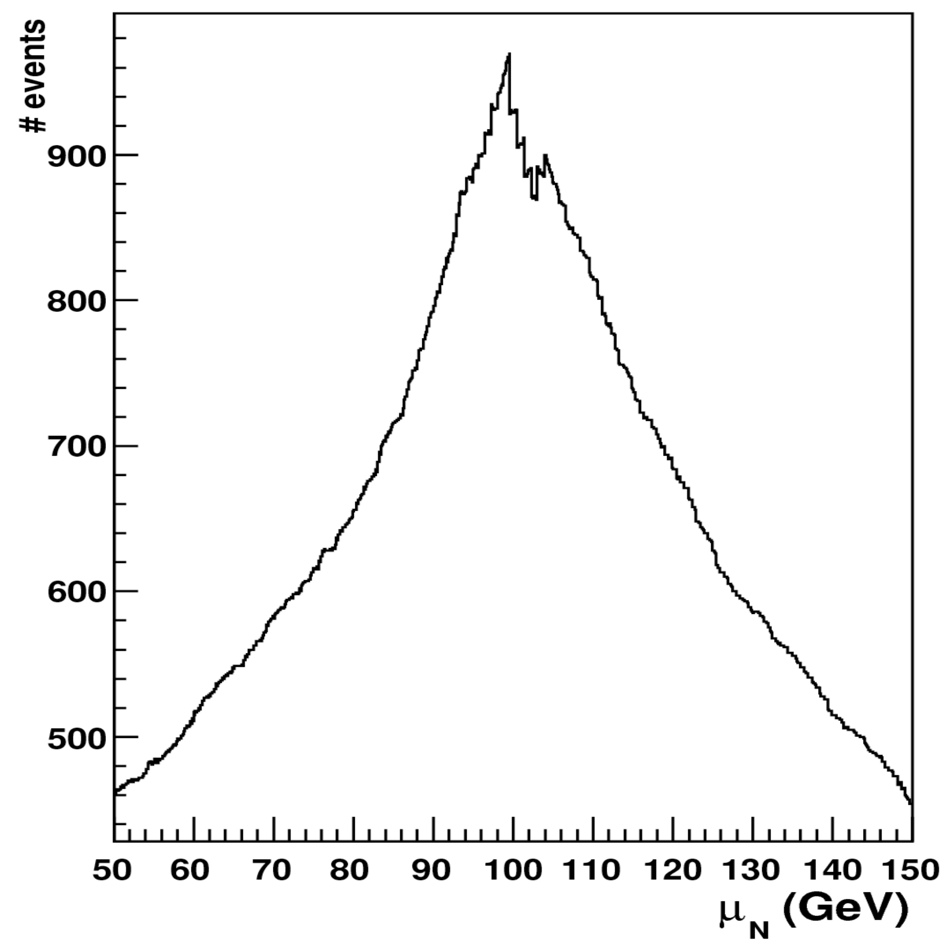

Conclusions

- A lot of progress in model-independent mass determination for invisible particles has been made recently.
- The relations among various kinematic variables and methods are better understood now.
- Combining these ideas together is likely to give the best determination of invisible particle masses.
- Event reconstruction can help to determine other properties (spins and couplings) of the new particles.